Research Article

International Journal of Advanced Technology and Engineering Exploration, Vol 12(123)
ISSN (Print): 2394-5443 ISSN (Online): 2394-7454
http://dx.doi.org/10.19101/IJATEE.2024.111100197

Addressing rutting damage in flexible pavements: a comprehensive analysis using finite element modelling and support vector machines

Amit Kumar[1], Rajesh Ranjan[2], Anish Kumar[1*] and Sanjeev Sinha[3]
Assistant Professor, Department of Civil Engineering, Rajkiya Engineering College, Azamgarh 276201, Uttar Pradesh, India[1]
Research Scholar, Department of Civil Engineering, National Institute of Technology Patna 800005, Bihar, India[2]
Professor, Department of Civil Engineering, National Institute of Technology Patna 800005, Bihar, India[3]

Received: 22-February-2024; Revised: 26-January-2025; Accepted: 09-February-2025

Abstract
The study aimed to investigate the rutting behaviour of the flexible pavement layers. Rutting is a significant distress mode in asphalt pavements, leading to severe serviceability issues. Understanding the rutting mechanisms in various pavement layers is crucial for improving pavement design and maintenance strategies. A three-dimensional finite element model (FEM) was constructed using the software ABAQUS to simulate the behaviour of flexible pavement layers under wheel loads. The study employed finite element analysis (FEA) to assess the rutting in different layers of the pavement structure. Additionally, support vector machine (SVM) models were constructed using the radial basis function (RBF) kernel to predict rutting behavior based on displacement data. The analysis revealed that the top layer of the pavement experienced a 3.8% reduction in rutting loss, while the subgrade layer showed only a 0.31% reduction. The top surface of the flexible (asphalt) pavement under the wheel load path experienced higher rutting than compressive stresses, which decreased laterally with horizontal distance. The critical rut depth was measured as 5.73 mm for the top layer and 3.8 mm for the base layer. The SVM models constructed with the RBF kernel function demonstrated superior performance, achieving R^2 values of 0.999 and 0.997 for displacement prediction at the center and edge of the pavement, respectively, under training conditions. The study demonstrated the effectiveness of FEA in evaluating the rutting behaviour of flexible pavement layers. The results highlighted the greater rutting in the top layer compared to the subgrade, emphasizing the need for focused attention on the top layers during pavement design and maintenance. Additionally, the SVM models with the RBF kernel accurately predicted pavement displacement, providing a valuable tool for future pavement analysis and optimization.

Keywords
Flexible pavement, Rutting behavior, ABAQUS, Finite element analysis (FEA), Support vector machine (SVM), Radial basis function (RBF) kernel.

1.Introduction
In traditional flexible pavements, a bituminous surface course is applied over a sub-base and base course, with one or more bituminous or hot mix asphalt (HMA) layers forming the surface path [1]. These pavements have low flexural strength and deform under applied loads, with the vehicle load directly affecting the surface course [2]. The load then distributes among base, sub-base, and subgrade courses, resembling a truncated cone. Asphalt pavement failure often results from increased traffic volumes and vehicle overloads, with rutting, a hazardous deformation, being a common consequence.

Rutting is characterized by permanent longitudinal grooves along the wheel path. It arises due to factors such as heavy channelized traffic, vehicle overloading, inadequate compaction during construction, unstable mix designs, weak pavement, soft or waxy bitumen, subgrade clay intrusion, or the use of plastic filler in granular sub-base (GSB), water bound macadam (WBM), or wet mix macadam (WMM) [3]. Rutting prevalence intensifies with increased heavy loads and road traffic, posing a significant challenge to asphalt pavement integrity.

Various laboratory tests, such as dynamic mechanical analysis, uniaxial repeated long creep testing, and wheel tracking tests, evaluate rutting failure [4]. Software tools such as IIT Pave, 3D-Move analysis,

*Author for correspondence

STAAD Pro, ABAQUS, ANSYS, PLAXIS-2D, and the mechanistic-empirical pavement design guide (MEPDG) support comprehensive rutting failure assessment [5]. Historically, the study of rutting behavior has primarily focused on the surface layer of asphalt pavements, often neglecting the complex interactions between the different layers of the pavement structure. Traditional methods of evaluating pavement performance have relied heavily on empirical data and field observations, which, while useful, offer limited insights into the intricate behaviors of individual pavement layers under various loading conditions [6, 7].

Recent advancements in computational modeling, however, have provided new avenues for more detailed analysis. Finite element analysis (FEA) using software like ABAQUS has become a powerful tool for simulating and analyzing the behavior of pavement structures under load. Despite these advancements, challenges remain in accurately modeling and predicting rutting behavior, especially when considering the interaction between different pavement layers and their respective contributions to overall performance. Many studies have been limited by their focus on either surface-level or subgrade behaviors, often neglecting the interactions between layers [4–9]. Furthermore, the prediction of rutting using traditional methods has been constrained by the lack of integration between empirical data and advanced analytical techniques.

The application of machine learning (ML) techniques, such as support vector machine (SVM), for predicting rutting behavior based on displacement data remains in its early stages, with few studies exploring the potential of these methods to enhance prediction accuracy. This study aims to bridge the gap by employing a comprehensive approach to evaluate rutting behavior across different flexible pavement layers. The primary objective is to investigate the rutting characteristics of various layers within the pavement structure using the three-dimensional FEA model. This model simulates the impact of wheel loads on the pavement, thus providing detailed insights into rutting behavior across different layers. Additionally, the study aims to develop and validate SVM models that use the radial basis function (RBF) kernel for predicting rutting behavior based on displacement data, thereby enhancing prediction accuracy and providing a valuable tool for future pavement analysis and design.

This paper is organized as follows: Section 2 discusses related work, Section 3 presents the materials and methods, and Section 4 covers the results and discussion. Finally, Section 5 provides the conclusion.

2.Literature review

Rutting in flexible pavements is a significant challenge, affecting their durability and serviceability. Traditional mechanistic-empirical approaches have been enhanced by advanced modeling techniques such as finite element modeling (FEM) and ML algorithms. ML techniques, including decision trees, random forests, SVM, and artificial neural networks (ANN), are widely used to predict fatigue cracking and rutting by analyzing large datasets containing material properties, traffic loads, and environmental conditions. The primary advantages of ML-based models include their ability to handle complex datasets and adaptability to different pavement conditions without requiring extensive recalibration. However, they require high-quality data and can be difficult to interpret [8].

Advanced sensors embedded in smart pavements have been explored for ML-based analysis. These sensors monitor real-time parameters such as stress, strain, temperature, and traffic loads, while ML techniques, including ANN, decision trees, and SVM, process this data to predict pavement performance. The benefits of this approach include real-time monitoring and predictive maintenance, which can reduce costs and extend pavement lifespan [9].

Research on rutting performance modeling in asphalt pavements includes empirical, mechanistic-empirical, and advanced computational approaches like FEA and ML. Traditional empirical models, based on historical data, are simple but often lack precision. Mechanistic-empirical models improve accuracy by incorporating material properties and loading conditions but require extensive calibration and validation. Advanced computational models, such as FEM, provide detailed simulations of pavement responses but demand significant computational power and expertise. While these models offer precise predictions and adaptability to various conditions, they require high-quality data and expert interpretation [10–12].

Artificial intelligence (AI) techniques in pavement engineering, such as ANN, SVM, decision trees, convolutional neural networks (CNNs), and recurrent neural networks (RNNs), learn from large datasets containing details on pavement materials, traffic conditions, and environmental factors. These AI models predict pavement deterioration, damage locations, and long-term structural integrity more accurately than traditional methods. AI's strengths include efficient data management, adaptability, and the ability to detect complex patterns. However, challenges include the need for high-quality data, risks of overfitting, and difficulties in interpreting complex AI models [13,14].

FEM and FEA are widely used to simulate pavement behavior under different loads and environmental conditions. These models accurately predict rut depth, stress distribution, and wear patterns, aiding in better pavement design and cost-effective maintenance. While requiring extensive data, computing power, and expert validation, FEM and FEA remain essential for designing long-lasting, high-performing roads [15–18].

A study [19] found that the distribution of horizontal tensile stress in the longitudinal direction correlates with cracking at the bottom of a U-shape, while the distribution pattern of horizontal shear stress in the longitudinal direction aligns with the bilateral areas of U-shaped cracking.

A comparative study [20] analyzed rutting in glazed asphalt pavement versus standard asphalt pavement. The results indicate that the proposed model reliably predicts rutting in asphalt mixtures. Additionally, it has been observed that vehicle overloading, along with tangential and vertical forces, significantly impacts rutting in asphalt pavements [21]. Another study [22] suggests that increasing rubber content to 10%, 15%, and 20% reduces rut depth by 41%, 56%, and 61% under static loading and by 40%, 55%, and 60% under repeated loading, respectively.

Table 1 summarizes key studies employing FEM and ML for rutting prediction, highlighting their methodologies, results, and limitations. These advancements demonstrate the potential of combining FEM with ML to improve rutting prediction accuracy and promote sustainable pavement management.

Table 1 Studies incorporating ML techniques

Objective	Methods	Results	Advantages	Limitations	Citation
To develop predictive models for fatigue cracking in flexible pavements using ML and to assess their performance compared to traditional empirical models.	Regression trees, SVM, ensemble trees, gaussian process regression (GPR), ANN, random forest algorithms were used to optimize the feature selection process.	In comparison to traditional empirical models, ML models performed better; ensemble trees had the greatest accuracy metrics root mean square error (RMSE) of 22.416, R^2 of 0.80848). Bayesian optimization enhanced the model's performance even further.	The study showed that ML models, which capture complex, non-linear interactions among factors, offer greater accuracy in fatigue cracking prediction. In pavement management, this method enables more accurate decision-making and resource allocation.	The representativeness and quality of the input data have a significant impact on the models. The significant computing resources needed to train these sophisticated ML models might be problematic for smaller datasets or organizations.	[23]
To investigate the use of ML algorithms for pavement performance monitoring and to provide affordable, competitive solutions for practical application in evaluating asphalt conditions"	SVM_S, random forest, ANN, CNN	Compared with traditional techniques, ML models shown promise in enhancing pavement performance evaluation's precision and effectiveness. While random forest worked well with numerical data, certain models, such as CNNs, proved useful for image-based crack identification.	ML gives scalable, precise, and effective ways to analyze large, complicated information. It makes automated, data-driven pavement management systems possible and lowers human error in inspections.	Pavement management organizations have not widely used ML models, which means that more model and data gathering needs to be improved.	[24]
The study aims to develop accurate rutting prediction models for asphalt pavements using ML methods, based on RIOHTrack data, to	SVM, ANN, gradient boosting decision tree (GBDT), random forest, extra trees	After random forest and extra trees, GBDT model has the highest R2 of 0.9835. In terms of rutting progression prediction, these models fared better than conventional	ML models were able to identify non-linear correlations in the data and showed excellent predicted accuracy. They may be used in real-world road	The models require substantial computational resources and high-quality data to be trained. Furthermore, they can only be used in situations when comparable datasets	[25]

Objective	Methods	Results	Advantages	Limitations	Citation
guide pavement maintenance and management decisions.		mechanistic-empirical models.	maintenance applications and need less calibration work than mechanistic-empirical models.	and attributes are accessible.	
The study aims at studying the effect of axle load increase, and the variation in pavement moduli, on the overall pavement life. It also aims to estimate the overweight truck limits that could be penalized or unloaded.	FEA using the ABAQUS software.	Vertical displacement is greatly decreased by increasing the thickness of the asphalt layer (for example, from 0.4178 mm to 0.0393 mm after 3600 seconds under a 54-ton load). Additionally, larger asphalt layers reduce vertical strains (from 7.518 kPa to 4.369 kPa). Durability is increased by thicker layers because they transfer less load to the underlying layers.	Finite element simulation is used to accurately simulate and analyze complicated phenomena. Useful advice on maximizing pavement thickness to lower maintenance costs and increase service life.	The results may not apply to different designs, loads, temperatures, or material properties since they are particular to the investigated conditions.	[26]
The study aims to analyze the performance of flexible pavement layers against rutting using FEM through ABAQUS software.	FEA using the ABAQUS software.	Maximum rut depth occurred at the center of the pavement width (137.594 mm). Due to the thicker binder course, the rut depth at 50 msa was 8.64% lower than at 10 msa.	Using FEM with ABAQUS offered detailed insights into stress distribution and deformation patterns, contributing to the optimization of pavement design.	The study did not consider factors such as temperature variations, moisture levels, and freeze-thaw cycles, which can greatly influence pavement performance.	[27]
The study reviews ML techniques for detecting and analyzing pavement distress, focusing on methods such as vibration, 2D, and 3D approaches to enhance road safety, reduce maintenance costs, and improve automated road monitoring systems.	CNN, Vibration-based approaches, Stereo vision techniques	The study demonstrates the efficacy of AI techniques in identifying cracks and potholes, with sophisticated approaches like as CNNs and 3D imagery reaching high accuracy and scalability for real-time applications.	Road networks are made safer and more resilient by automated detection, which also greatly lowers manual labor, improves accuracy, and permits effective repair scheduling.	Existing systems have issues with noisy environments, little datasets, and practical application, especially under different lighting and weather situations.	[28]
To evaluate the accuracy, dependability, and usefulness of several predictive models for asphalt pavement rutting, including mechanical, empirical, ML, and combination techniques.	A comprehensive review of literature and a practitioner survey were conducted to analyze various model types, including their parameters, strengths, and limitations, for rutting prediction.	The study emphasized the significance of integrating field data with sophisticated modeling tools for more accurate forecasts, highlighting developments in predictive modeling for rutting.	Improves pavement management by combining several modeling techniques to offer insights into rutting processes and prediction accuracy.	The models' general applicability and real-world application under many settings are limited by their frequent reliance on particular conditions, datasets, and assumptions.	[29]
To develop and compare ML models for predicting asphalt pavement rutting using the long-term pavement performance (LTPP) database, enhancing accuracy in diverse climatic and structural conditions.	Regression decision trees, SVM, ensemble tree, GPR, ANN	The most accurate ML method was GPR, which outperformed other methods with an R^2 of 0.70 and a RMSE of 1.96.	The study offers reliable and accurate rutting prediction models, which use cutting-edge AI algorithms to lower maintenance costs and support pavement management choices.	Performance may differ under unmodeled environmental or structural circumstances, and the models rely on the quality and availability of large datasets.	[30]
To analyze factors affecting pavement	Random Forest, light gradient boosting	Rutting reduces with vehicle speed but rises	It combines ML with FEM to provide a	Results are limited in their ability to be	[31]

Objective	Methods	Results	Advantages	Limitations	Citation
rutting in Pakistan by using FEM and ML models, focusing on variables like temperature, speed, and loading cycles.	machine (LGBM), AdaBoost, Linear regression	with temperature and loading cycles. With precise rutting predictions, LGBM outperformed the other ML models.	rigorous study that provides insights to forecast rutting, improve road design, and increase sustainability.	generalized under different real-world circumstances since they are dependent on controlled simulations and particular datasets.	

This research aims to analyze the rutting behavior of different flexible pavement layers using FEA. The data for this study has been sourced from secondary references, specifically IRC-37:2018 and the Ministry of Road Transport and Highways (MORTH) guidelines. FEA is a numerical technique that decomposes complex engineering problems into smaller, more manageable components. It is widely used for rutting prediction [32], stress analysis [33], material characterization [34], and cost-effectiveness evaluation [35].

In addition to the FEA of the rutting behavior of the flexible pavement layers, an SVM-based ML prediction model was developed to predict displacement at the center and edge of the pavement. The dependent variable in this study is pavement displacement, while pavement layer depth is considered the independent variable. The SVM model incorporates various kernel functions, including RBF, linear, and polynomial kernels, to enhance prediction accuracy.

3.Methods

The focus of the work is the development of an FEA framework for analyzing the rutting behavior of flexible pavement. The methodology used in the current study is presented in *Figure 1*. This paper presents a new method for characterizing the rutting of flexible pavements using a creep model-based FEA model. The study also investigated the effects of rutted pavement and high tire pressure on pavement performance.

New standards for determining the failure of pavement layers were developed based on the analysis of transverse surface profiles. Creep deformation refers to the gradual increase in material deformation over time under constant temperature and stress. At moderate temperatures, asphalt mixtures behave as viscoelastic substances and can exhibit significant creep. In this study, a creep model was implemented in FEA to simulate the behavior of viscoelastic asphalt mixtures.

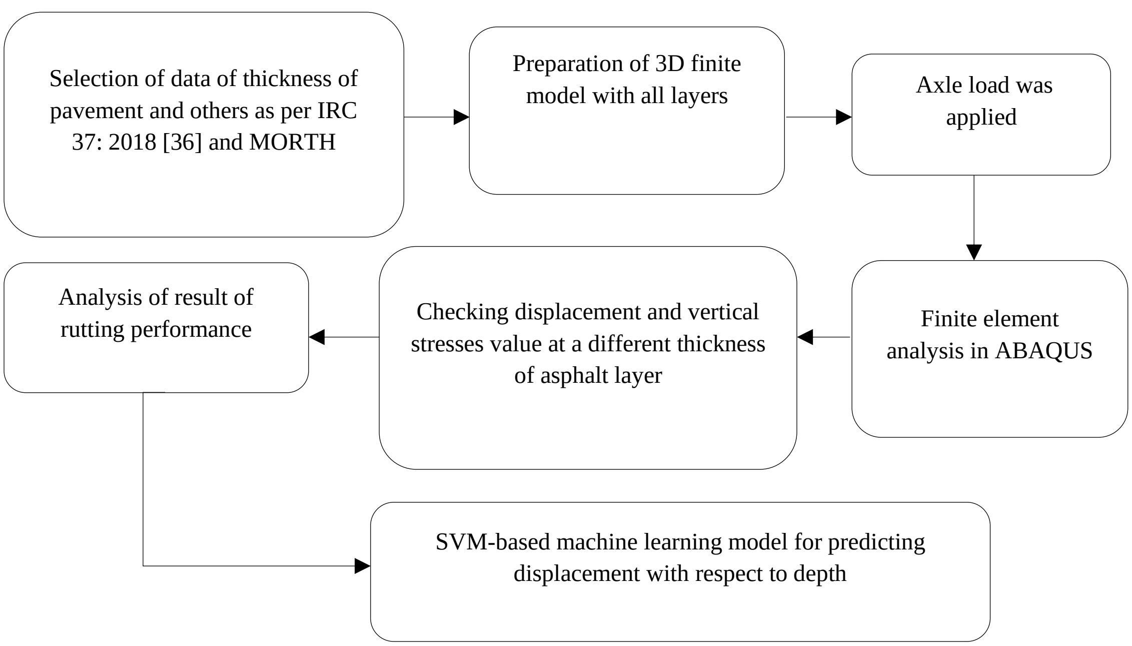

Figure 1 Methodology of the study

Under normal temperatures, the asphalt mixture is just a viscous elastic material that could creep significantly. The total strain (ε_t) of the material is decomposed to elastic strain (ε_e) & non-elastic strain (ε_{in}) to explain its creep behavior, that is,

$$\varepsilon_t = \varepsilon_e + \varepsilon_{in} \tag{1}$$
$$\varepsilon_{in} = \varepsilon_p + \varepsilon_c \tag{2}$$

where, ε_p =plastic strain and ε_c =creep strain used in Equations 1 and 2.

If the pavement has still not yet reached the yield phase due to the wheel load effect, then ε_p=0 and ε_t could be described as follows as per Equation 3.

$$\varepsilon_t = \varepsilon_e + \varepsilon_c \tag{3}$$

Where ε_c has nothing to do with time. The relationship among ε_c and strain σ & ε_c and elastic modulus (*E)* can be presented in Equation 4:

$$\varepsilon_e = \frac{\sigma}{E} \tag{4}$$

ε_c is a function of time t, T (temperature), & σ.

$$\varepsilon_c = f(t,T,\sigma) = f_1(t) f_2(T) f_3(\sigma) \tag{5}$$

At constant temperature, ε_c as per Equation 5 can be expressed as follows if the asphalt mix is experiencing major creep due to the wheel loading.

$$\varepsilon c = f(t,\sigma) = \frac{A}{m+1}\,\sigma^n t^{m+1} \tag{6}$$

Where, creep parameters of the material are A, m, and n. The specific parameters of the creep model (A, m, n) are crucial for understanding how materials deform over time under constant load conditions, especially when predicting pavement rutting. Parameter "A" indicates how sensitive the material is to stress during the creep process, reflecting its creep compliance. The value of parameter A varies depending on the material type and application, determined through material testing and specific calibration. Parameter m relates to how the material's creep rate changes with stress levels, indicating stress dependency. For many materials, parameter m typically falls between 3 and 5, with higher values indicating more sensitivity to stress. Parameter n describes how the material's creep strain rate changes over time, reflecting time dependency. Materials exhibiting viscoelastic behavior often have parameter n between 3 and 6, with higher values indicating a more pronounced time-dependent response. These parameters are fundamental in developing creep models that accurately predict how materials will deform over extended periods under load. Their selection involves material testing, empirical data, and calibration to ensure the models correctly represent the material's behavior. In this study, the creep model parameters (A, m, and n) were not calibrated through experimental testing. Instead, the model utilizes parameter values derived from secondary sources, such as the IRC-37:2018 [36] and MORTH guidelines, which are based on extensive field data and prior research in pavement engineering. These sources provide standard values for asphalt mixture behavior under typical loading and temperature conditions, which are commonly used in the initial stages of pavement modeling. The primary goal of this study was to develop and present a methodology for simulating rutting behavior in flexible pavements using a creep-based FEA model, rather than to perform a detailed calibration of the material parameters. Calibration of the creep model would require extensive laboratory testing and field data collection, which was outside the scope of this work. The parameters used in this study are intended to provide a preliminary framework for modeling pavement deformation, with the understanding that future research should focus on the experimental determination and fine-tuning of these parameters for more accurate predictions of pavement behavior under specific conditions. Equation 6 is the time differential equation that can be used to calculate the creep strain rate.

$$\frac{d\varepsilon c}{dt} = A\,\sigma^n t^m \tag{7}$$

Equation 7 is the creep model's time hardening formula, which is widely used in creep analysis during constant load. The creep model's strain hardening formula is widely used for creep studies under non-constant loads.

$$\frac{d\varepsilon c}{dt} = \{A\sigma^n [(m+1)\,\varepsilon_c]^m\}^{1/m+1} \tag{8}$$

Thus, in equation 8, the creep strain rate is proportional to the cumulative values of creep strain although not to the passage of time. The creep law of the asphalt mixture should be chosen as equation viii for pavement rutting prediction under moving load. Other pavement components in the existing model were considered to be isotropic as well as linear elastic in this work.

The development of the creep model-based FEA for simulating rutting behavior in flexible pavements involved several key preprocessing steps and assumptions that helped simplify the complex system while ensuring the model's practicality and relevance to real-world pavement design. The geometry of the pavement layers, including the asphalt surface, base, sub-base, and subgrade, was defined based on typical cross-sections found in highway pavements. The pavement layers were modeled with quadratic hexahedral finite elements, with mesh refinement applied near the tire contact area to capture the stress gradients accurately. The pavement was assumed to be fixed at the bottom, representing the subgrade, and wheel loads were applied at the top surface, both at the center and edge of the pavement, to simulate typical traffic loading scenarios. Several assumptions were made to simplify the modeling process. First, the non-asphalt layers (base, sub-base, and subgrade) were assumed to behave as linear elastic, isotropic materials, with constant elastic moduli based on IRC-37:2018 [36] and MORTH guidelines. This assumption was made to focus the study on the creep behavior of the asphalt mixture and its role in rutting. The asphalt mixture was modeled as a viscoelastic material, with both elastic and time-dependent creep behavior, following a creep law based on a power-law function. This function was used to describe the asphalt's deformation under sustained loads, with material parameters.

A, m, and n selected from secondary sources and literature, as no experimental calibration was conducted in this study. The creep parameters were chosen based on typical values for asphalt mixtures, with A reflecting the material's sensitivity to stress, m indicating the material's stress dependency, and n capturing the time-dependent behavior. Since calibration was not performed, these parameters were selected from common ranges found in previous research and established pavement design standards. The input parameters for the model, including elastic moduli, Poisson's ratios, and creep parameters, were chosen based on typical values derived from IRC-37:2018 [36] and other relevant standards. The choices made in the preprocessing and parameter selection were justified based on the need to create a manageable yet realistic model that could provide useful insights into the rutting behavior of flexible pavements. By using standard material properties and simplifying the pavement structure, the model could focus on understanding the long-term deformation behavior of the asphalt under typical loading conditions. The assumptions about linear elasticity for non-asphalt layers and constant temperature were made to reduce the model's complexity, while the use of secondary data for creep parameters was deemed appropriate given the lack of direct calibration data. While these assumptions helped make the study feasible, further calibration with experimental data would enhance the model's accuracy and provide more reliable predictions for specific pavement types and traffic conditions. The data has been taken from secondary sources IRC-37:2018 [36] and MORTH guidelines. The input parameters of the pavement layer are presented in *Table 2*, while the corresponding properties are detailed in *Table 3*. *Figures 2*, *3*, and *4* illustrate the subgrade, sub-base, and base layers developed in ABAQUS, respectively. *Figure 5* depicts the axle load applied at the center of the pavement model, whereas *Figure 6* shows the axle load applied at the edge of the pavement model.

Table 2 Input parameters of pavement layer

Pavement layer	Layer thickness (mm)	Resilient modulus (MPa)	Density (Kg/m)	Poisson ratio
Modified Bitumen Mix	150	3000	2246	0.35
Granular Base	260	359	2120	0.35
Granular Sub-base	250	147	2120	0.35
Subgrade	500	61.14	1960	0.35

Table 3 Properties of pavement layer

Thickness of the pavement	Subgrade CBR	Poisson ratio	M_R (MPa)
1160 mm	> 5% (7% taken)	0.35	$17.6 * (CBR)^{0.64} = 61.14$

The pavement structure described in the current study consists of multiple layers, each with distinct material properties and characteristics that contribute to the overall performance of the pavement. The layers include a modified bitumen mix, granular base, granular sub-base, and subgrade, each serving a specific function in distributing loads, providing stability, and ensuring durability. The modified bitumen mix forms the topmost layer (150 mm thick) and serves as the wearing course of the pavement. This layer is characterized by a high resilient modulus (3000 MPa), indicating its rigidity and ability to resist deformation under traffic loads. The material's density is 2246 kg/m³, and a Poisson's ratio of 0.35 is assumed, which is typical for bituminous materials. The high resilient modulus reflects the stiff, load-bearing nature of the bitumen mix, which is crucial for maintaining surface integrity under traffic loads and providing a smooth, durable riding surface. The granular base layer, with a thickness of

260 mm, is located beneath the bitumen mix and provides structural support to the pavement. It has a resilient modulus of 359 MPa, which is lower than that of the modified bitumen but still significant for load distribution. This layer is typically composed of crushed stone or gravel, with a density of 2120 kg/m³ and a Poisson's ratio of 0.35. Granular materials are used for their ability to transfer load effectively and to provide drainage within the pavement structure. The granular sub-base layer, 250 mm thick, sits beneath the granular base and further contributes to load distribution and drainage. Its resilient modulus is 147 MPa, indicating a softer material compared to the granular base, yet still adequate for supporting traffic loads. Like the granular base, the sub-base has a density of 2120 kg/m³ and a Poisson's ratio of 0.35. The sub-base is typically made of coarse aggregates, sand, or gravel, which allow water to drain away from the pavement structure, preventing moisture-related damage.

Finally, the subgrade layer, the deepest and thickest (500 mm), consists of natural soil and is crucial for providing foundational support to the entire pavement system. The resilient modulus for the subgrade is calculated using the empirical formula given in *Table 3*, with a California bearing ratio (CBR) of 7%, yielding a resilient modulus of 61.14 MPa. The subgrade typically has a lower stiffness compared to the upper layers, reflecting its natural, variable properties. Its density is 1960 kg/m³, and the Poisson's ratio is assumed to be 0.35. The subgrade is often the most variable layer in terms of material properties, depending on the soil type, moisture content, and compaction, and is a critical factor in determining the overall performance of the pavement structure.

The material properties of these layers are primarily sourced from secondary references such as the IRC-37:2018 [36] and MORTH guidelines, which provide standard values for various pavement materials used in road construction. In the absence of direct experimental data for some of these materials, reasonable assumptions were made based on typical values for each material type in similar pavement designs. For instance, the Poisson's ratio of 0.35 is a common assumption for granular materials and bituminous mixes, reflecting their typical behavior under stress. The resilient modulus values are derived from empirical relationships and standard design methodologies for road pavements. Together, these layers are designed to interact effectively under traffic loading conditions, with each layer playing a key role in ensuring the longevity and load-carrying capacity of the pavement. The model setup, which includes axle loads applied both at the center and the edge of the pavement, helps simulate real-world loading conditions, ensuring that the design can withstand a range of stresses from traffic and environmental factors.

Boundary condition

FEA is a versatile technique for solving a series of differential equations over a field, with the solution satisfying defined boundary conditions. The boundary condition at the bottom – restricted in X, Y, and Z directions against displacement. In the boundary condition at the bottom and the type of the model is Symmetry/ Anti-symmetry/ Encastre in which the boundary condition should be: ENCASTRE (U1 = U2 = U3 = UR1 = UR2 = UR3 = 0), where U_1 represents displacement in the x-direction, U_2 represents displacement in the y-direction, U_3 represents displacement in the z-direction, UR1 represents displacement rotation in X direction, UR2 represents displacement rotation in X direction, UR3 represents displacement rotation in X direction. *Figure 7* depicts the boundary conditions of flexible pavement. *Figure 8* depicts the boundary condition at the bottom of flexible pavement.

Support vector machine (SVM)

SVM based regression is a powerful and versatile ML technique used for predictive modeling and regression analysis [37–41]. Unlike traditional linear regression, SVM regression seeks to find a nonlinear mapping of the data, allowing it to capture complex relationships between variables. In the context of regression, the goal of SVM is to find the optimal hyperplane that best fits the data by maximizing the margin between the data points and the hyperplane, while also minimizing the margin violations, often referred to as "support vectors." This hyperplane is defined as in Equation 9:

$$y(x)=w^{T}\cdot x + b \tag{9}$$

Here, $y(x)$ represents the predicted output, x is the input feature vector, w is a weight vector that determines the orientation of the hyperplane, and b is a bias term. The SVM regression objective is to minimize the following cost function:

$$min_{w,b,\epsilon}\frac{1}{2}||\mathrm{w}||^2 + \mathrm{c}\sum_{i=1}^{n}\epsilon_I \tag{10}$$

The Equation 10 balances the trade-off between minimizing the norm of w and minimizing the margin violations (quantified by ϵ) with a regularization parameter c. SVM-based regression is a valuable tool for tasks where traditional linear regression is insufficient, as it can handle complex, non-linear relationships between input and output variables.

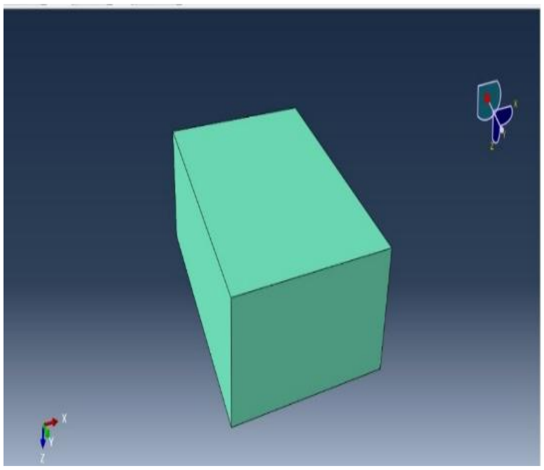

Figure 2 Subgrade layer built on ABAQUS

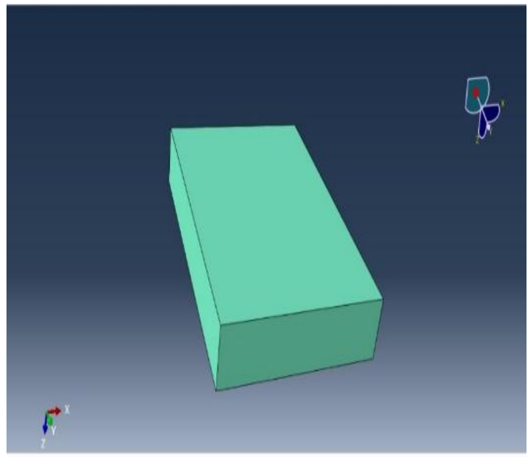

Figure 3 Sub-base layer built on ABAQUS

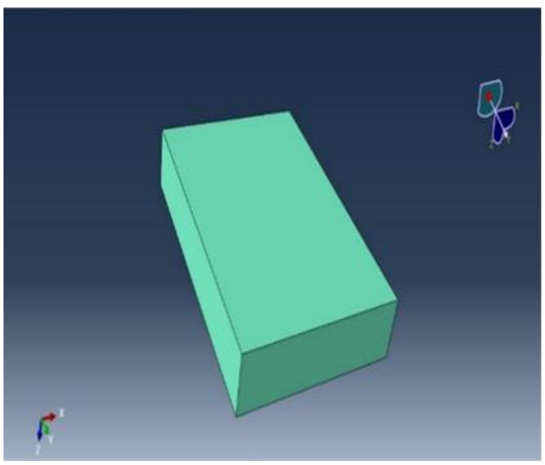

Figure 4 Base layer built on ABAQUS

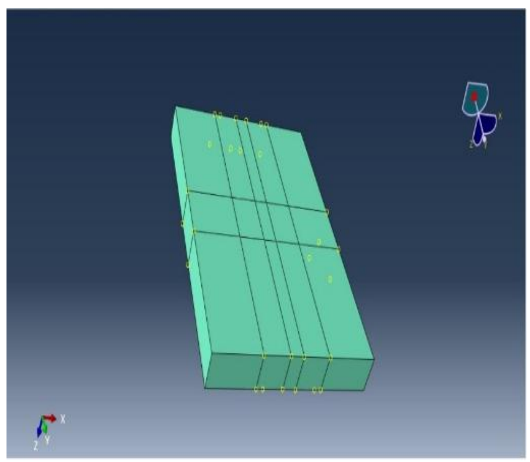

Figure 5 Asphalt layer-load applied at the centre

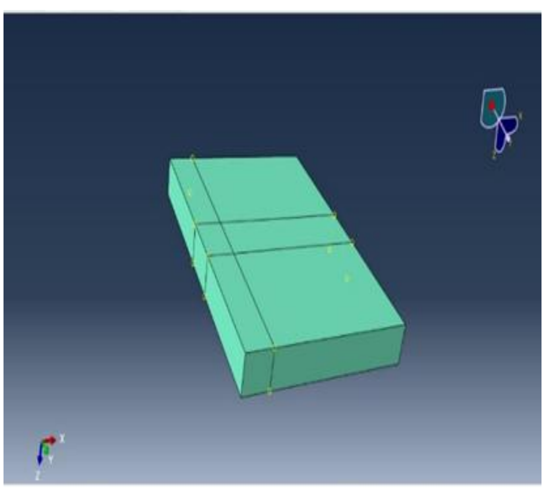

Figure 6 Asphalt layer-load applied at the edge

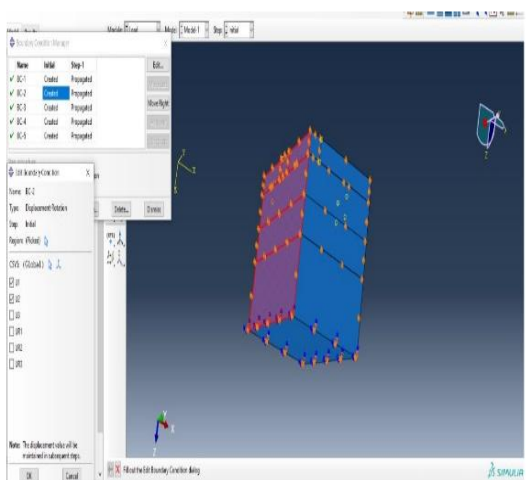

Figure 7 Boundary conditions of flexible pavement

4.Results and discussion

This section contains a comprehensive discussion on the results obtained after analyzing the FEA model on ABAQUS.

4.1Effect of load applied at the center of the pavement model

The lower portion of the subgrade is fixed, which ensures that the nodes just at the bottom of the subgrade can't shift up and down (vertically and horizontally). *Figure 9* shows the pavement layers with their respective boundary conditions. Its boundary nodes along its pavement edges become restricted horizontally, although they are freely able to move vertically. The study used the ABAQUS three-dimensional solid-element library's 8-node quadrilateral plane strain element. To improve accuracy, all elements were biquadratic with 8 nodes. A series of finite element analyses were conducted with the element size decreasing to determine the optimal mesh size. A fine mesh is used all over the loading area along the wheel path in both vertical & horizontal directions, and a coarse mesh has been used well belonging from the loading area. The mesh had a total of 1936 elements and 1670 nodes. The meshing conditions and nodes are shown in *Figure 10*. The mesh statistic is shown in *Figure 11*.

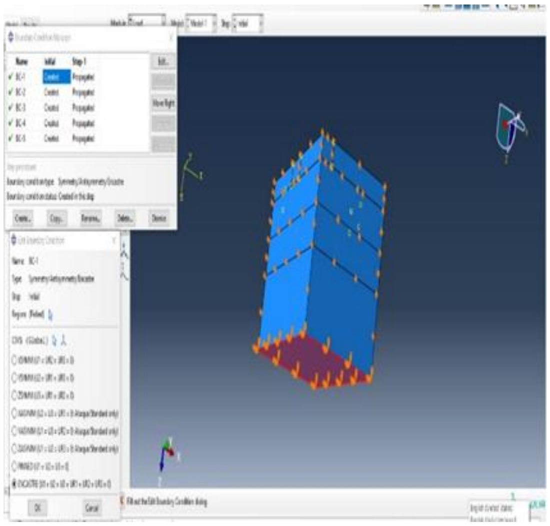

Figure 8 Boundary condition at the bottom of flexible pavement

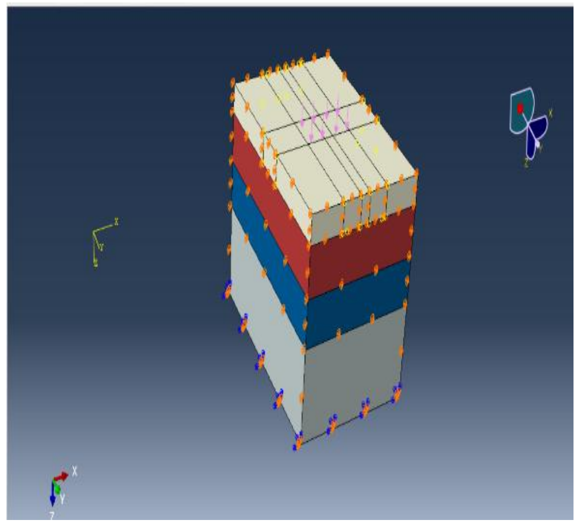

Figure 9 Pavement layers with boundary conditions (load at centre)

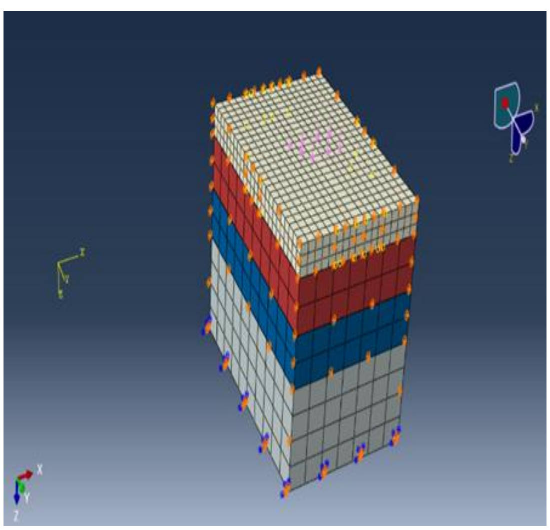

Figure 10 Pavement layer with meshing conditions

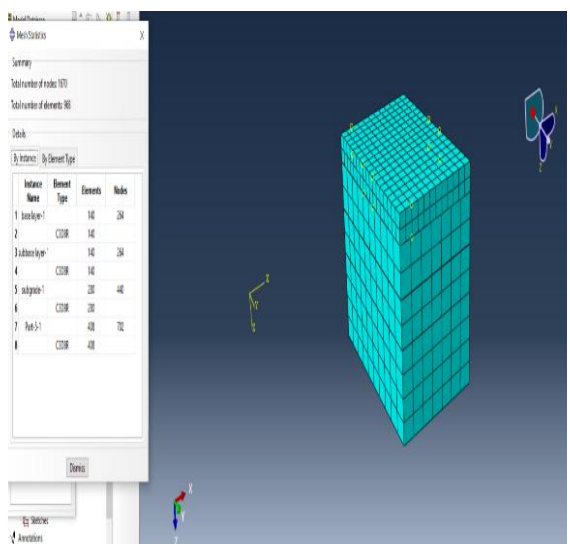

Figure 11 Mesh Statistics (Load at center)

On the application of the load at the center of the pavement model, it gets deflected from the top layers to the bottom respectively. Indications of different colors (*Figure 12*) show the defection of each layer from top to bottom. The asphalt layer gets more defects in comparison to the subgrade layer as shown in *Figure 12* and *Figure 13* shows the stress distribution in the different pavement layers. *Figure 14* shows the displacement v/s depth plot observed in the pavement with load at the center.

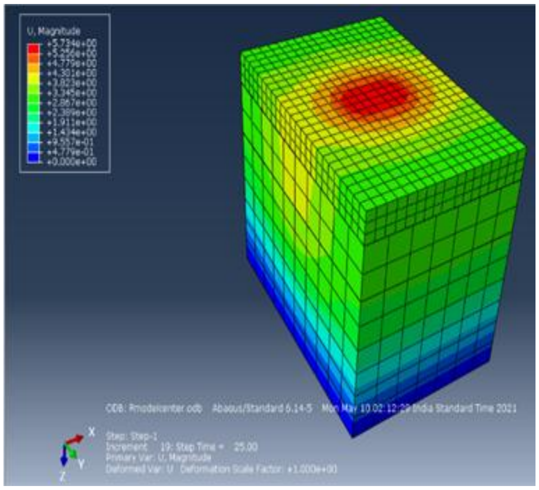

Figure 12 Rutting in the pavement with modified bitumen (Load at centre)

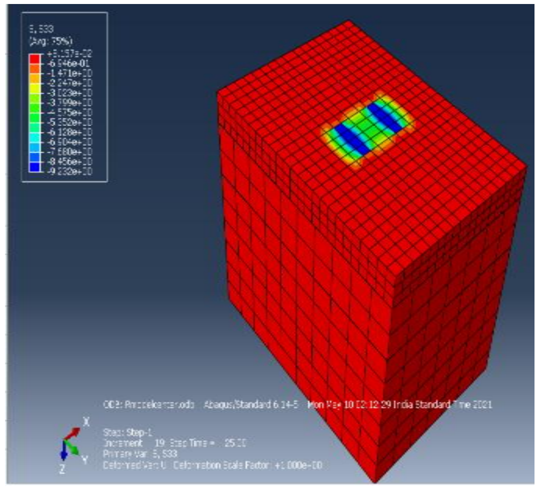

Figure 13 Stresses in the pavement with modified bitumen (Load at centre)

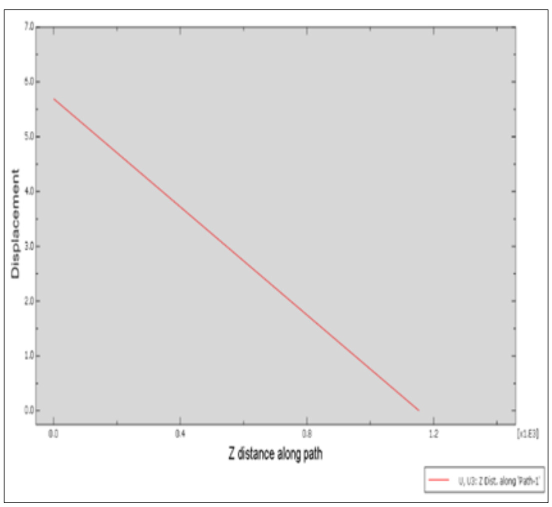

Figure 14 Displacement v/s Depth plot (Load at centre)

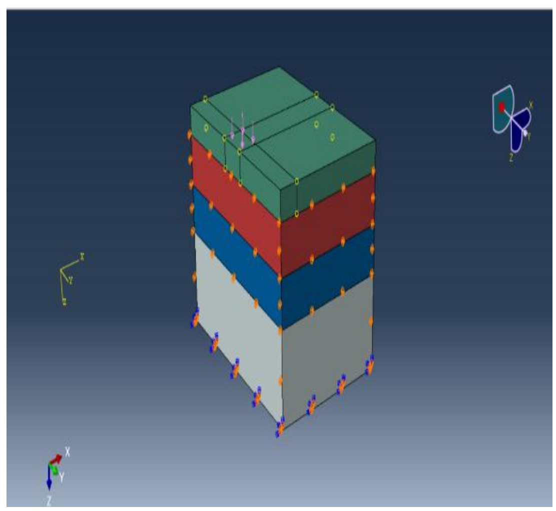

Figure 15 Pavement layer with Boundary conditions (load at edge)

4.2Effect of load applied at the edge of the pavement model

The lower portion of the subgrade is fixed, which ensures that the nodes just at the bottom of the subgrade can't shift up and down (vertically and horizontally). *Figure 15* shows the pavement layers with their respective boundary conditions. Its boundary nodes along its pavement edges become restricted horizontally, although they are freely able to move vertically. The study used the ABAQUS three-dimensional solid-element library's 8-node quadrilateral plane strain element. To improve accuracy, all elements were biquadratic with 8 nodes. A series of finite element analyses were conducted with the element size decreasing to determine the optimal mesh size. The meshing conditions and nodes are shown in *Figure 16*. The mesh statistic is shown in *Figure 17*. On the application of load at the edge of the pavement model, it gets deflected from the top layer to the bottom respectively. Indications of different colors show the defection of each layer from top to bottom. The asphalt layer gets more defects in comparison to the subgrade layer. *Figure18* shows the rutting in the pavement with modified bitumen. *Figure 19* shows the stress distribution in the different pavement layers. *Figure 20* shows the displacement v/s depth plot observed in the pavement with load at the edge. The total depth of the pavement is 1160 mm in which bitumen layer thickness is 150 mm, granular base layer thickness is 260 mm, granular sub base (GSB) layer thickness is 250 mm and thickness of subgrade layer is 500 mm. Total rut depth when load is applied at the centre and edge is 5.73 and 6.17 respectively. According to the result, deflection of layers from top to bottom is decreasing. Pavement design intentionally causes the deflection to decrease from top to bottom. It guarantees that the lower layers of the road provide the structural integrity and load-bearing capacity required to sustain the traffic loads over time, while the road surface may give comfort and safety for cars. Sustaining the lifespan and functionality of the road requires this layering of materials with different stiffness qualities.

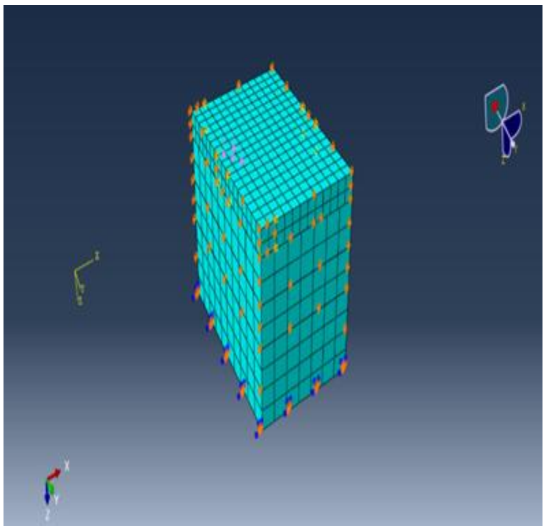

Figure 16 Pavement layer with meshing conditions (load at edge)

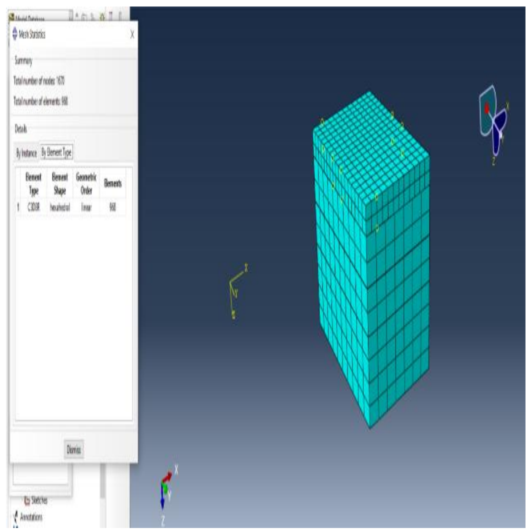

Figure 17 Mesh Statistics (load at edge)

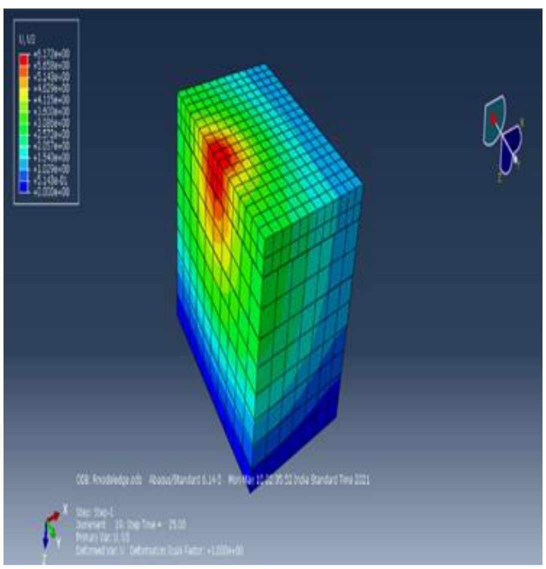

Figure 18 Rutting in the pavement with modified bitumen (load at edge)

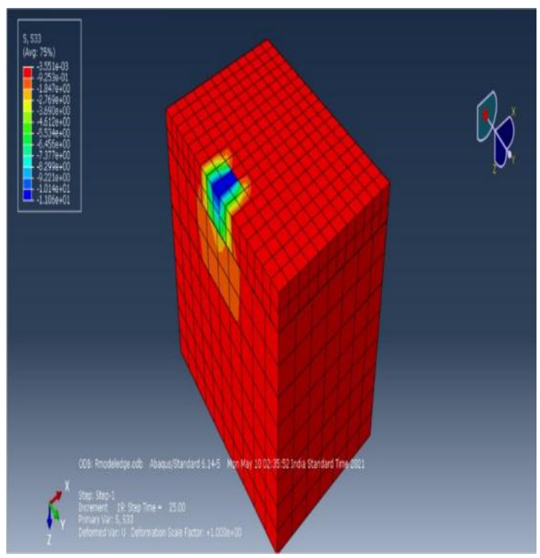

Figure 19 Stresses in the pavement with modified bitumen (load at edge)

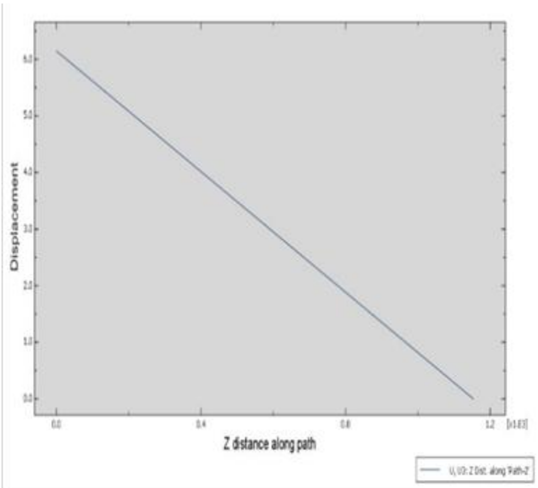

Figure 20 Displacement v/s Depth plot (load at edge)

4.3SVM based ML model

Three SVM models based on different kernel functions were developed in the current study. The three kernel functions used in the study were (i) RBF (ii) linear and (iii) polynomial. Predictive models for displacement at centre and edge of the pavement were developed in the current study. The data obtained from FEA was divided into training and testing databases. The descriptive statistics of the training and testing dataset used in the current study is shown in *Table 4* and *Table 5* respectively.

Preparing data for an SVM model involves several key preprocessing steps to ensure optimal performance. First, data cleaning is conducted to handle missing values, outliers, and any inconsistencies. Next, standardization is a crucial preprocessing step since SVMs are sensitive to the scale of the input features. Standardization transforms the data to have a mean of zero and a standard deviation of one, ensuring that all features contribute equally to the model and preventing bias toward features with larger magnitudes. Following this, feature selection or engineering is performed to identify and retain only the most relevant predictors, potentially improving the model's performance and interpretability. Finally, the dataset is split into training and testing subsets to allow for model validation and performance evaluation.

Different kernel functions are chosen in SVM to handle various types of data distributions and complexities. The linear kernel is suitable for linearly separable data, as it finds a hyperplane with minimal computational cost. The RBF kernel is widely used for non-linear problems due to its ability to map input features into a higher-dimensional space, capturing complex patterns in the data. The polynomial kernel is beneficial when the relationship between features is non-linear but follows a polynomial structure, allowing for flexibility with different degrees of polynomial transformations. Choosing the appropriate kernel depends on the data's underlying structure and the problem's requirements.

Hyperparameter tuning is essential for optimizing SVM performance, and cross-validation is a commonly used method for this purpose. Cross-validation splits the dataset into multiple folds, training the model on a subset while validating it on the remaining data. This process is repeated for all folds, ensuring robust evaluation by reducing the risk of overfitting. For hyperparameter tuning, grid search is often employed in conjunction with cross-validation, systematically exploring combinations of key parameters such as the regularization parameter C, the kernel-specific parameters (e.g., gamma for RBF), and the degree of the polynomial kernel. This ensures that the model achieves the best balance between bias and variance, ultimately improving generalization on unseen data.

The training and testing dataset must be derived from the same population distribution so that the model accurately depicts the true characteristics of the data used in the study. A Kolmogorov-Smirnov (KS) test was used for this purpose. The null hypothesis and alternate hypothesis for the KS test is "H_0*: The two samples follow the same distribution*" and "H_a*: The distributions of the two samples are different*" respectively. The results (*Table 6*) shows that the training and testing dataset have the same population distribution in both the cases as the computed p-value is greater than the significance level alpha=0.05, thus the null hypothesis H_0 in each case cannot be rejected. The cumulative distribution of the training and testing datasets for centre and edge models is shown in *Figure 21.*

In the current study a 10-fold cross validation was employed. K-fold cross-validation is employed in ML to robustly assess a model's performance. It divides the dataset into K subsets, training and testing the model K times, using each subset as the test set once. This minimizes data leakage, efficiently utilizes available data, and offers a more reliable estimate of a model's ability to generalize. It aids in hyper parameter tuning, provides insights into model consistency, and quantifies confidence in performance metrics. K-fold cross-validation is a key practice to mitigate overfitting, improve model selection, and ensure a model's reliability when faced with new, unseen data. The results of the 10-fold cross validation (*Table 7*) study show that in almost all the subsets the models performed with substantial accuracy which is highlighted by high coefficient of determination (R^2) and low mean squared error (MSE).

The parameters of the SVM model hyper tuned using trial and error method. The hypertuned parameters of the SVM models developed in the study are listed in *Table 8*. The performance comparison (*Table 9*) of SVM kernel functions reveals that the RBF kernel consistently outperforms both the linear and polynomial kernels across all metrics. For mean absolute error (MAE), the RBF kernel achieves the lowest values, with 0.043 (training) and 0.048 (testing) in the center region, compared to significantly higher values for the linear and polynomial kernels, which reach 0.191 (training) and 0.254 (testing).

A similar trend is observed for MSE, where the RBF kernel records minimal values of 0.002 (training) and 0.003 (testing) in the center region, whereas the Linear and Polynomial kernels exhibit much larger errors, such as 0.054 (training) and 0.080 (testing). Root mean squared error (RMSE) also highlights the RBF kernel's superior performance, with the lowest values in both regions. Most notably, the RBF kernel achieves near-perfect R^2 values of 0.999 (training) and 0.998 (testing) in the center region and similarly high results in the edge region, significantly outperforming the linear and polynomial kernels, whose R^2 values drop as low as 0.954 during testing in the center region. The RBF kernel's success stems from its flexibility to capture nonlinear patterns by mapping inputs into a higher-dimensional feature space, allowing it to handle the complex relationships within the data effectively. This adaptability contrasts sharply with the limitations of the linear kernel, which assumes strict linearity, and the polynomial kernel, which may require higher degrees for comparable performance, increasing computational costs and the risk of overfitting. Additionally, the RBF kernel demonstrates robustness across different data regions, maintaining consistently low errors and high R^2 values in both center and edge regions. This scalability is achieved through hyperparameter tuning, such as optimizing the gamma parameter, which enables the kernel to generalize well. In contrast, the simpler functional forms of the linear and polynomial kernels restrict their performance, particularly in regions with nonlinear characteristics, such as the center. Overall, the RBF kernel's ability to balance model complexity and generalization while avoiding overfitting makes it the most effective choice for this dataset.

The correlation plot shown for the SVM models developed in the study for the centre and edge is shown in *Figure 22* and *Figure 23* respectively. It is clearly evident from *Figure 22 (a)* and *Figure 24 (a)* that the majority of points in both training and testing datasets align to the 45-degree line in the SVM models developed with RBF kernel function. Taylor's diagram and Box and whiskers plot were also drawn to understand the robustness of different models developed in the study. The Taylor's diagram of various SVM models for the center and edge is shown in *Figure 23* and *Figure 25* respectively. It is seen in all the Taylor diagrams that the SVM model developed using RBF kernel function is visually close to the observed dataset as compared to other SVM model. This inference also adds to the robustness of the RBF based SVM model.

Box and whisker plot for the SVM model of center and edge of the pavement is shown in *Figure 26*. These plots are used to understand the distribution of errors in prediction by the various models developed in the study. The smallest interquartile range was observed for RBF based SM models for center and edge. In comparison to other models, the shorter interquartile range indicates less variability in the error distribution. This also indicates to a robust RBF based SVM model.

Table 4 Descriptive statistics of the training dataset used in the study

Location	Variable	Observations	Minimum	Maximum	Mean	Std. deviation
Centre	Displacement (mm)	32	0.000	5.716	3.228	1.967
	Depth (mm)	32	0.000	1154.390	585.310	373.362
Edge	Displacement (mm)	32	0.000	6.146	3.192	1.851
	Depth (mm)	32	0.000	1153.850	576.026	337.954

Table 5 Descriptive statistics of the training dataset used in the study

Location	Variable	Observations	Minimum	Maximum	Mean	Std. deviation
Centre	Depth (mm)	10	115.439	1010.090	585.851	253.078
Edge	Depth (mm)	10	115.385	1125.010	580.133	393.001

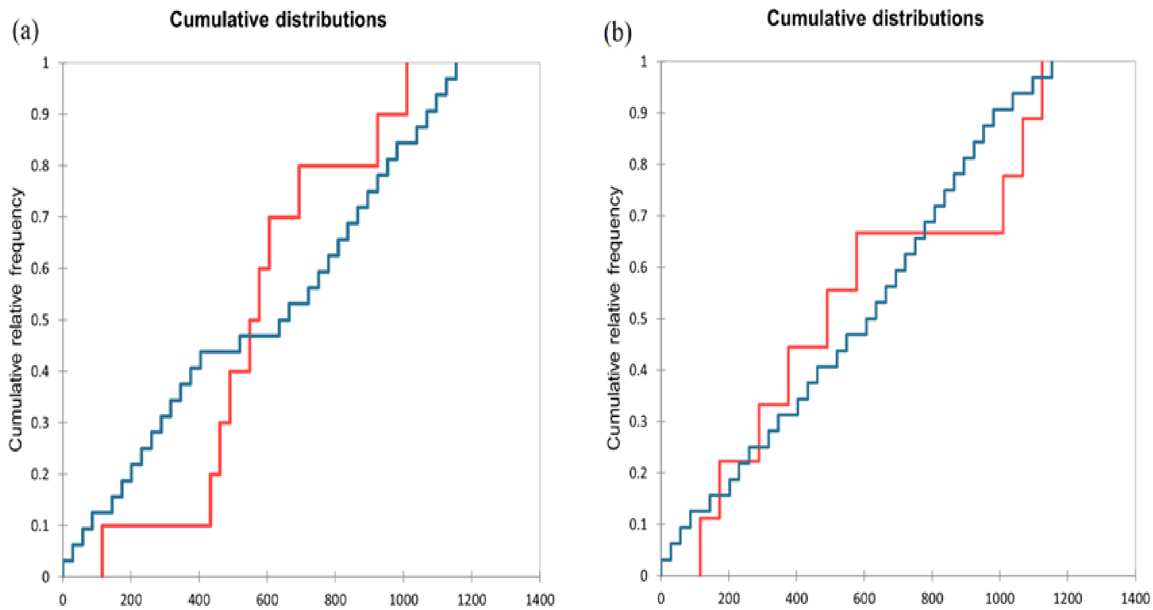

Figure 21 Cumulative distribution of training and testing dataset: (a) Centre (b) Edge (Blue: Training, Red: Testing)

Table 6 Two-sample Kolmogorov-Smirnov (KS) test

Statistic	Centre	Edge
D	0.338	0.240
p-value (Two-tailed)	0.286	0.727
alpha	0.05	0.05

Table 7 Cross validation results

Model		Metric	K-Fold									
			1	2	3	4	5	6	7	8	9	10
RBF	Center	MSE	0.006	0.016	0.005	0.001	0.003	0.004	0.008	0.002	0.001	0.001
		R^2	0.999	0.997	0.977	0.999	0.998	0.998	0.998	0.999	0.999	0.999
		MAE	0.068	0.075	0.059	0.025	0.047	0.062	0.075	0.039	0.026	0.025
	Edge	MSE	0.03	0.02	0.004	0.012	0.019	0.008	0.057	0.01	0.001	0.001
		R^2	0.992	0.994	0.997	0.994	0.991	0.996	0.988	0.989	0.999	0.976
		MAE	0.145	0.135	0.06	0.115	0.117	0.077	0.177	0.078	0.017	0.03
Linear	Center	MSE	0.044	0.011	0.075	0.203	0.074	0.077	0.184	0.014	0.044	0.102
		R^2	0.966	0.997	0.984	0.986	0.964	0.973	0.961	0.993	0.992	0.974
		MAE	0.172	0.096	0.271	0.142	0.205	0.255	0.335	0.105	0.193	0.279
	Edge	MSE	0.005	0.012	0.015	0.279	0.019	0.006	0.033	0.019	0.023	0.012
		R^2	0.985	0.996	0.997	0.992	0.99	0.941	0.963	0.995	0.946	0.997
		MAE	0.062	0.105	0.121	0.116	0.109	0.076	0.175	0.114	0.148	0.078
Polynomial	Center	MSE	0.08	0.02	0.136	0.062	0.217	0.037	0.019	0.073	0.052	0.056
		R^2	0.981	0.994	0.977	0.963	0.882	0.99	0.729	0.976	0.975	0.977
		MAE	0.235	0.101	0.341	0.22	0.147	0.185	0.132	0.242	0.199	0.144
	Edge	MSE	0.022	0.279	0.032	0.026	0.338	0.008	0.026	0.004	0.009	0.014
		R^2	0.994	0.995	0.989	0.994	0.997	0.998	0.986	0.987	0.996	0.968
		MAE	0.144	0.167	0.159	0.137	0.581	0.085	0.118	0.059	0.071	0.108

Table 8 Hyper tuned parameters of SVM models

SVM-Kernel	RBF		Linear		Polynomial	
Attribute	Centre	Edge	Centre	Edge	Centre	Edge
Bias	-0.153	-0.020	-0.006	0.023	-0.006	0.023
Number of support vectors	11	5	15	5	15	5
C	100	100	1	1	1	1
Epsilon	0.03	0.1	0.01	0.01	0.1	0.1
Tolerance	0.001	0.001	0.001	0.001	0.001	0.001
γ	1	0.5	-	-	0.5	0.5
Degree	-	-	-	-	1	1
Coefficient	-	-	-	-	0	0
Preprocessing	Standardization					

Table 9 Performance metric of SVM models (Displacement in mm)

SVM Kernel		Metric	MAE	MSE	RMSE	MSLE	RMSLE	R^2
RBF	Center	Training	0.043	0.002	0.048	0.000	0.017	0.999
		Testing	0.048	0.003	0.053	0.000	0.015	0.998
	Edge	Training	0.084	0.011	0.104	0.002	0.042	0.997
		Testing	0.083	0.010	0.098	0.001	0.038	0.998
Linear	Center	Training	0.191	0.054	0.233	0.006	0.078	0.986
		Testing	0.254	0.080	0.284	0.005	0.067	0.954
	Edge	Training	0.110	0.016	0.125	0.003	0.052	0.995
		Testing	0.108	0.015	0.122	0.004	0.066	0.996
Polynomial	Center	Training	0.191	0.054	0.233	0.006	0.078	0.986
		Testing	0.254	0.080	0.284	0.005	0.067	0.954
	Edge	Training	0.110	0.016	0.125	0.003	0.052	0.995
		Testing	0.108	0.015	0.122	0.004	0.066	0.996

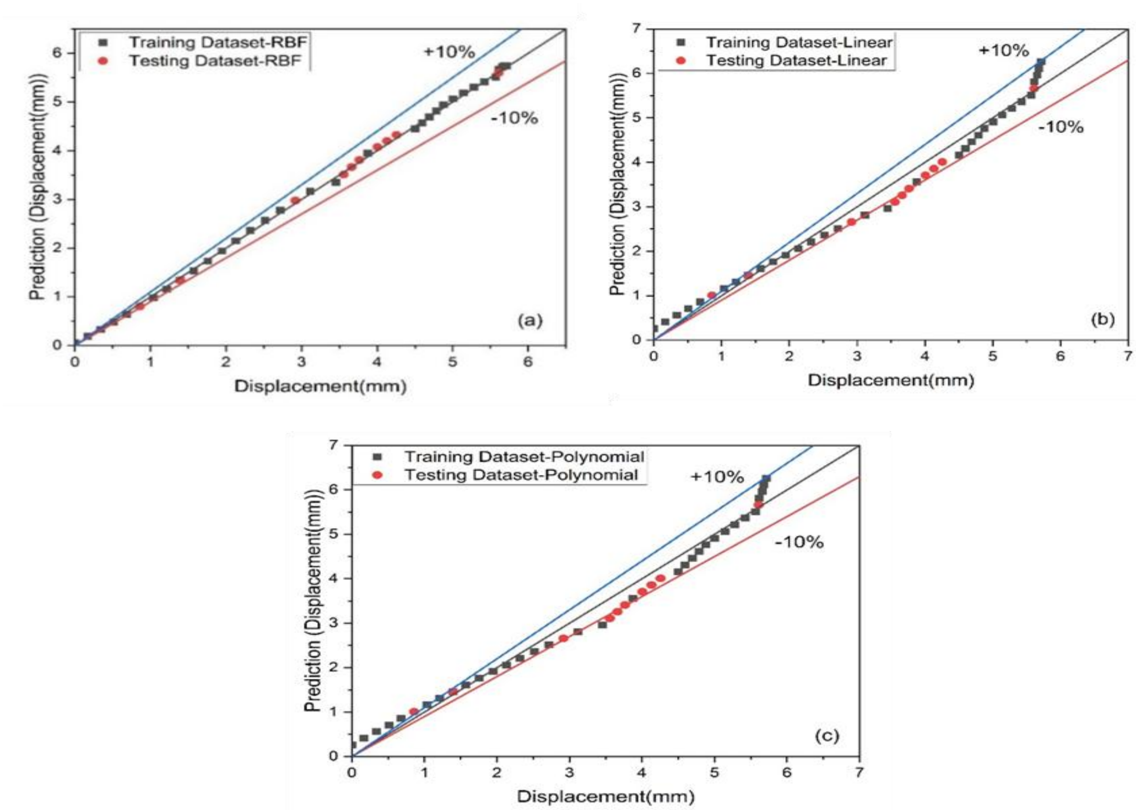

Figure 22 Correlation plots for SVM models at center: (a) RBF (b) Linear (c) Polynomial

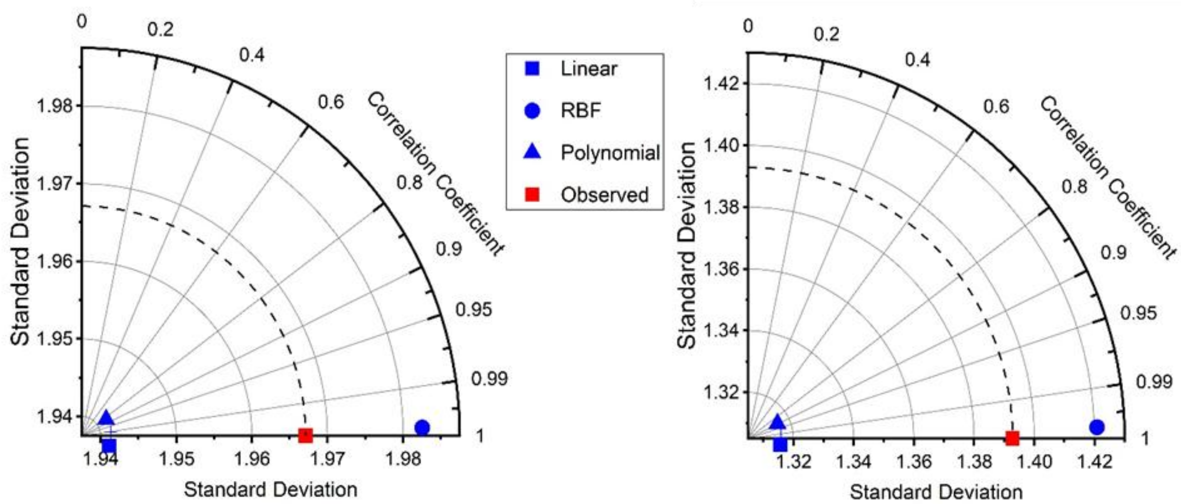

Figure 23 Taylor's diagram for SVM models at center: (a) Left: Training (b) Right: Testing

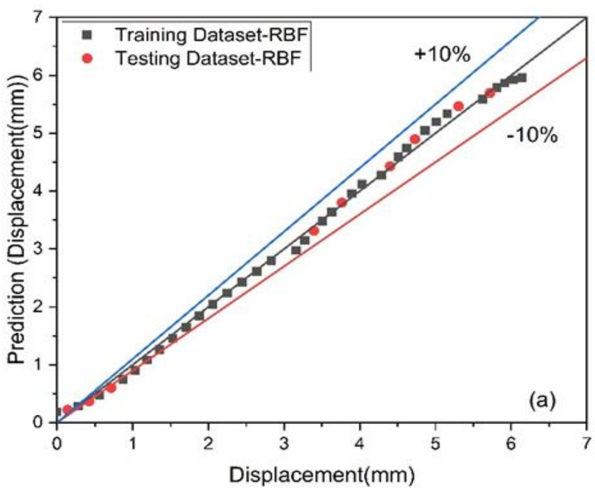

(a)

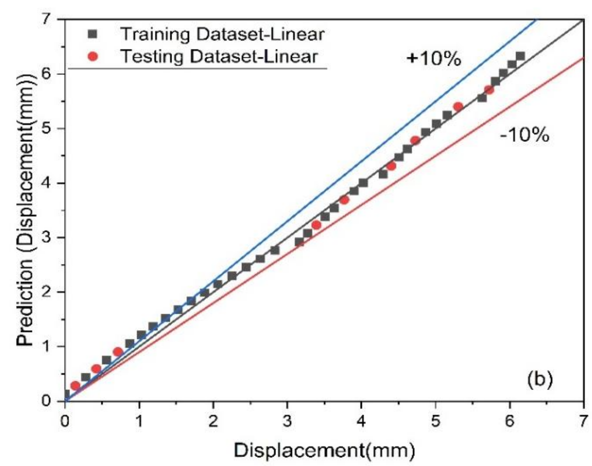

(b)

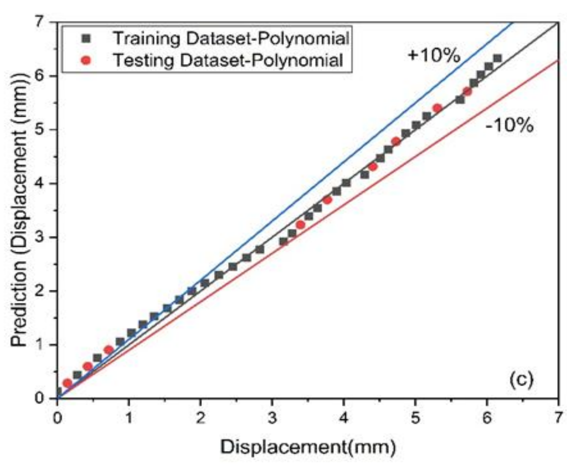

(c)

Figure 24 Correlation plots for SVM models at edge: (a) RBF (b) Linear (c) Polynomial

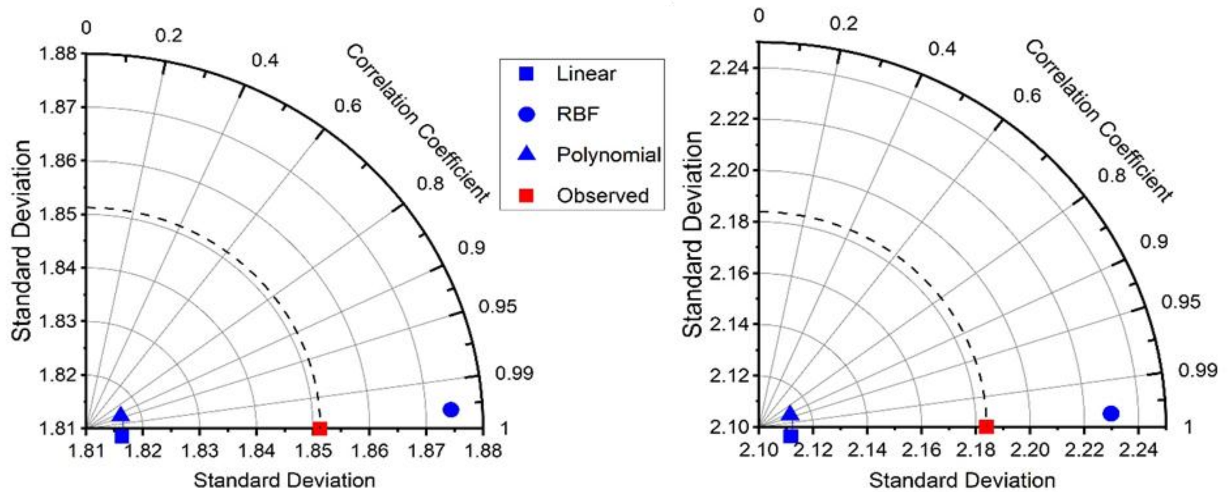

Figure 25 Taylor's diagram for SVM models at edge: (a) Left: Training (b) Right: Testing

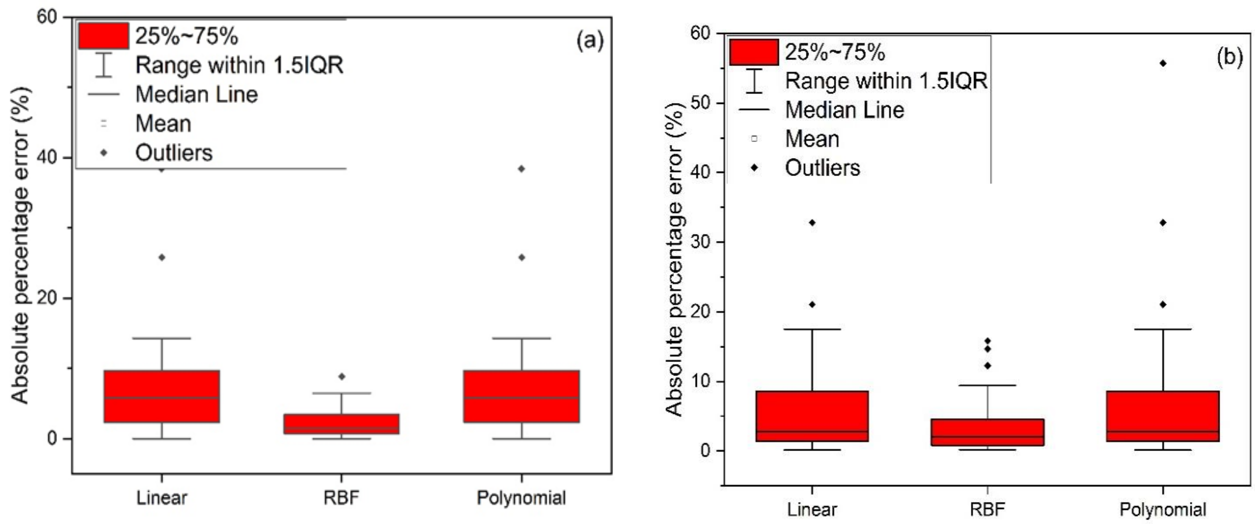

Figure 26 Box and whisker plot (a) Left: SVM model for center (b) Right: SVM model for center Testing (training dataset)

4.4Error analysis for SVM kernel functions

An error analysis of the SVM model using different kernel functions highlights distinct patterns in the distribution and magnitude of errors across metrics and data regions. The following breakdown examines these errors in detail to understand the model's behavior and areas for improvement.

Error magnitude (MAE and RMSE)

The RBF kernel demonstrates the lowest error magnitudes in both the center and edge regions, with MAE of 0.043 (training) and 0.048 (testing) in the center region, and 0.084 (training) and 0.083 (testing) in the edge region. These values indicate that the average prediction error is minimal and consistent across regions, suggesting that the RBF kernel captures the underlying data patterns effectively. In contrast, the linear and polynomial kernels exhibit significantly higher MAE values, particularly in the center region, where the testing MAE reaches 0.254. This suggests that these kernels struggle to model the more complex or nonlinear relationships present in the data. Similarly, RMSE, which penalizes larger errors more heavily, shows that the RBF kernel has far smaller deviations (e.g., 0.048 training RMSE for center) compared to the linear and polynomial kernels (0.233 training RMSE for center). The large RMSE for linear and polynomial kernels indicates that occasional large errors skew the overall prediction accuracy.

Squared errors (MSE and MSLE)

MSE confirms the patterns observed with RMSE, showing the RBF kernel achieving minimal squared error values (0.002 training, 0.003 testing for center), while Linear and Polynomial kernels exhibit values over an order of magnitude larger in the same region (0.054 training, 0.080 testing). Mean squared logarithmic error (MSLE) and its square root (RMSLE) further highlight the RBF kernel's ability to minimize logarithmic deviations, which is critical for datasets with large target ranges. Linear and Polynomial kernels, despite their poor performance in linear-scale metrics, exhibit similar MSLE performance, suggesting limited suitability for large-value predictions.

Model generalization (R^2)

The RBF kernel achieves near-perfect R^2 scores in both center (0.999 training, 0.998 testing) and edge regions (0.997 training, 0.998 testing). These values indicate that the RBF kernel captures nearly all the variance in the data, confirming its robustness and reliability. The linear and polynomial kernels, however, show significantly lower R^2 values in the center region, particularly during testing (0.954). This drop highlights a generalization issue, where these kernels fail to adapt to the complexity of the center region's data. In the Edge region, the R^2 scores for linear and polynomial kernels improve (0.996), likely due to a simpler relationship between input and output variables.

Data region-specific observations

In the center region, the errors are consistently lower for the RBF kernel, suggesting that it effectively captures the complex and possibly nonlinear patterns in this region. Linear and polynomial kernels show significantly higher error metrics, indicating an inability to model the complexity inherent in the data. In the edge region, all kernels perform better in this region, the RBF kernel still achieves the lowest errors. The linear and polynomial kernels, however, exhibit marginally closer performance to the RBF kernel, likely due to simpler relationships in this subset of data.

Potential Causes of Errors

RBF Kernel: The errors for the RBF kernel are minimal but not zero, suggesting room for further hyperparameter optimization (e.g., gamma and C). These small errors might also stem from noise or outliers in the dataset. The higher errors for these kernels indicate a fundamental mismatch between their functional assumptions and the data's underlying patterns. The linear kernel struggles with nonlinearities, while the polynomial kernel may require higher degrees to achieve similar performance, risking overfitting or computational inefficiency.

Recommendations for improvement

In case of RBF Kernel, fine-tuning of hyperparameters using grid search or Bayesian optimization may further reduce errors. Techniques such as feature scaling and noise reduction in the dataset can also help. In case of linear and polynomial kernels, feature engineering can be considered to better linearize the data or exploring higher-degree Polynomial kernels. Alternatively, adopting hybrid models that combine linear and nonlinear approaches might address their limitations.

The RBF kernel demonstrates superior performance due to its ability to handle nonlinearities and generalize across different data regions. Linear and Polynomial kernels are less effective, particularly in regions requiring complex modelling, and would benefit from additional feature transformations or more advanced configurations.

4.5Practical implications of the study

The findings of this study, particularly the use of a creep model-based FEA to simulate rutting behavior in flexible pavements, have significant practical implications for pavement design and maintenance. The observed stress distributions within the pavement structure offer valuable insights into how different factors, such as traffic loads, tire pressure, and temperature, affect the long-term performance of pavements. By identifying high-stress zones and areas of stress concentration near the tire-pavement contact point, the model helps inform better design practices, especially in regions with high traffic volumes or heavy vehicle loads. This understanding enables more effective pavement layer design by optimizing materials and thicknesses to distribute stresses evenly and reduce rutting risk in vulnerable areas. The model also highlights the importance of selecting appropriate asphalt mixtures that can resist deformation under sustained loads, which can guide material selection based on expected traffic conditions.

Furthermore, the study's findings emphasize the need for tailored designs in areas subject to heavy loads and high tire pressures, such as truck routes or urban roads. Pavements in such regions may require greater thickness or more durable materials to withstand the higher localized stresses and mitigate premature failure. The model's ability to predict the progressive deformation of asphalt mixtures over time also provides critical insights for maintenance planning, enabling engineers to anticipate when and where rutting is likely to occur, thereby optimizing rehabilitation schedules and reducing long-term maintenance costs. By understanding the time-dependent creep behavior of asphalt, engineers can design pavements that perform better over their lifecycle, minimizing the need for frequent repairs and extending the lifespan of the pavement.

The study also provides guidance for updating pavement design codes, considering stress distributions and factors such as tire pressure and temperature. These insights could lead to the development of more precise load distribution factors and recommendations for layer thicknesses based on specific traffic conditions, ensuring that pavements are more resilient under varying environmental and load conditions. This study provides a comprehensive framework for improving pavement design, maintenance, and rehabilitation practices, leading to more durable and cost-effective pavements that perform well under modern traffic loads.

4.6Limitations of FEA based rutting model

While FEA is a valuable tool for modelling pavement rutting behaviour, it has limitations when applied to real-world conditions. FEA often relies on simplified material models and assumptions about material properties, which do not fully capture the complex, time-dependent, and temperature-sensitive behaviour of pavement materials like asphalt. Additionally, FEA models typically use static or quasi-static loading conditions which do not account for the dynamic and variable nature of real-world traffic loads. Assumptions regarding boundary conditions and the uniformity of pavement sections can further reduce the prediction accuracy, as real pavements experience varying subgrade conditions, and environmental factors. The high computational demands of detailed FEA models can also limit their application, making it challenging to simulate long-term pavement performance. Moreover, the lack of extensive field data for validation and the challenges in calibrating FEA models to real-world conditions introduce uncertainties in their predictive capabilities. Factors like temperature fluctuations and moisture effects are often oversimplified, potentially leading to inaccuracies. Given these limitations, while FEA provides valuable insights, it should be used in conjunction with empirical models, field data, and real-world testing for a more accurate assessment of rutting behaviour. A complete list of abbreviations is listed in *Appendix I.*

5.Conclusion and future work

Given the improved accuracy of FEA, a finite element-based model was developed to better understand the rutting behavior of different flexible pavement layers. The total thickness of the flexible pavement layer is 1160 mm, and the load was applied at the center of the pavement, the rutting of the asphalt layer was reduced by 5.73 mm from the top while rutting damage on the subgrade layer was reduced by 0.47 mm from the bottom. The rutting damage of the asphalt layer was reduced by 6.17 mm, while the rutting damage of the subgrade layer was reduced by only 0.51 mm only when the load was applied at the edge of the pavement. A lower rut value indicates that less maintenance is required, which in turn extends the pavement's lifespan. Permanent deformation across the bottom, intermediate, and top pavement layers is uneven, with rutting predominantly caused by deformation in the intermediate pavement layer. Controlling the permanent deflection of the intermediate pavement layer should be a key factor in enhancing the anti-rutting capability of the pavement. According to FEM analysis, maximum rutting depth occurs under static loading conditions. SVM models using RBF, linear, and polynomial kernel functions were developed to predict displacement at the center and edge of the pavement. The SVM models developed using RBF kernel function outperformed other SVM models. The R2 value for the RBF kernel-based SVM model for displacement at centre and edge of the pavement is 0.999 and 0.997 respectively in training conditions. The closely packed correlation plot for both the models also adds to the robustness of the model. The robustness of the RBF-based SVM model is further validated using Taylor's diagram and a box-and-whisker plot. Based on the results, it can be concluded that the application of SVM-like ML algorithms can robustly depict the rutting behaviour of flexible pavements and thus the use of other ML algorithms falls under the future scope of work.

Acknowledgment

None.

Conflicts of interest

The authors have no conflicts of interest to declare.

Data availability

The data will be made available by the corresponding author upon reasonable request.

Author’s contribution statement

Amit Kumar: Writing – original draft, Writing – review and editing. **Rajesh Ranjan**: FEA analysis, Writing –

review and editing. **Sanjeev Sinha:** Conceptualization and review. **Anish Kumar:** Writing – review and editing.

References

[1] Mensahn ES, Wada SA, Lugeiyamu L. Structural evaluation of conventional and modified flexible pavement performance. Arid Zone Journal of Engineering, Technology and Environment. 2021; 17(4):535-46.

[2] Al-taher MG, Sawan AM, Solyman ME, El-sharkawi Attia MI, Ibrahim MF. Evaluating the durability of asphalt mixtures for flexible pavement using different techniques: a review. International Journal of Pavement Research and Technology. 2024:1-27.

[3] Kou B, Cao J, Huang W, Ma T, Shi Z. Rutting prediction model of asphalt pavement based on RIOHTrack full-scale ring road. Measurement. 2025; 242:115915.

[4] Alamnie MM. Laboratory-based study of viscoelastic, viscoplastic and fatigue damage of asphalt concrete. Doctoral Thesis, University of Agder. 2024.

[5] Patel VJ, Juremalani J, Kumavat HR. Incorporation of high volume ground granulated slag from blast furnaces in pavement quality concrete. Engineering, Technology & Applied Science Research. 2024; 14(4):14888-93.

[6] Zhang AA, Shang J, Li B, Hui B, Gong H, Li L, et al. Intelligent pavement condition survey: overview of current researches and practices. Journal of Road Engineering. 2024; 4(3): 257-81.

[7] Li Q, Xiao DX, Wang KC, Hall KD, Qiu Y. Mechanistic-empirical pavement design guide (MEPDG): a bird’s-eye view. Journal of Modern Transportation. 2011: 114-33.

[8] Gong H, Sun Y, Hu W, Huang B. Neural networks for fatigue cracking prediction using outputs from pavement mechanistic-empirical design. International Journal of Pavement Engineering. 2021; 22(2):162-72.

[9] Kang J. Pavement performance prediction using machine learning and instrumentation in smart pavement. Master's Thesis, University of Waterloo. 2022.

[10] Liu Y, You Z, Li L, Wang W. Review on advances in modeling and simulation of stone-based paving materials. Construction and Building Materials. 2013; 43:408-17.

[11] Deng Y, Shi X. Short-term predictions of asphalt pavement rutting using deep-learning models. Journal of Transportation Engineering, Part B: Pavements. 2024; 150(2):04024004.

[12] Bayat R, Talatahari S, Gandomi AH, Habibi M, Aminnejad B. Artificial neural networks for flexible pavement. Information. 2023; 14(2):1-23.

[13] Yang X, Guan J, Ding L, You Z, Lee VC, Hasan MR, et al. Research and applications of artificial neural network in pavement engineering: a state-of-the-art review. Journal of Traffic and Transportation Engineering (English Edition). 2021; 8(6):1000-21.

[14] Mikels N, Kassem E, Muftah A, Sufian AA. The Use of Artificial Intelligence in Pavement Engineering. Pacific Northwest Transportation Consortium (PacTrans) (UTC); 2023.

[15] Kotb MM. Prediction of distresses in pavement networks: a machine learning approach. Master's Thesis, The American University in Cairo (Egypt). 2024.

[16] Karadag H, Firat S, Isik NS, Yilmaz G. Determination of permanent deformation of flexible pavements using finite element model. Građevinar. 2022; 74(6):471-80.

[17] Pandey AK, Mathur D. Finite element analysis and optimization of flexible pavement. International Journal of Civil Engineering Applications Research. 2023; 4(1):6-25.

[18] Deng Y, Zhang Y, Shi X, Hou S, Lytton RL. Stress–strain dependent rutting prediction models for multi-layer structures of asphalt mixtures. International Journal of Pavement Engineering. 2022; 23(8):2728-45.

[19] Liu L, Hao P. ABAQUS program-based numerical analysis on U-shaped cracking of asphalt pavement. In international conference on remote sensing, environment and transportation engineering 2011 (pp. 2861-4). IEEE.

[20] Arabani M, Jamshidi R, Sadeghnejad M. Using of 2D finite element modeling to predict the glasphalt mixture rutting behavior. Construction and Building Materials. 2014; 68:183-91.

[21] Al-khateeb LA, Saoud A, Al-msouti MF. Rutting prediction of flexible pavements using finite element modeling. Jordan Journal of Civil Engineering. 2011; 5(2):173-90.

[22] Imaninasab R, Bakhshi B, Shirini B. Rutting performance of rubberized porous asphalt using finite element method (FEM). Construction and Building Materials. 2016; 106:382-91.

[23] Alnaqbi AJ, Zeiada W, Al-khateeb G, Abttan A, Abuzwidah M. Predictive models for flexible pavement fatigue cracking based on machine learning. Transportation Engineering. 2024; 16:1-24.

[24] Cano-ortiz S, Pascual-muñoz P, Castro-fresno D. Machine learning algorithms for monitoring pavement performance. Automation in Construction. 2022; 139:1-16.

[25] Cheng C, Wang L, Zhou X, Wang X. Predicting rutting development using machine learning methods based on RIOCHTrack data. Applied Sciences. 2024; 14(8):1-21.

[26] Alwan DS, Joni HH, Hilal MM. Deformation behavior of flexible pavements by finite element simulation. Periodicals of Engineering and Natural Sciences (PEN). 2022; 10(6):142-50.

[27] Kumar P, Kiran KBV, Manjunatha S, Subramanya KG. Finite element modeling by ABAQUS for rutting in flexible pavement. Civil Engineering and Architecture. 2024; 12(3):1576-84.

[28] Kothai R, Prabakaran N, Murthy YS, Cenkeramaddi LR, Kakani V. Pavement distress detection, classification and analysis using machine learning algorithms: a survey. IEEE Access. 2024; 12:126943-60.

[29] Deng Y, Shi X. Modeling the rutting performance of asphalt pavements: a review. Journal of Infrastructure Preservation and Resilience. 2023; 4(1):1-21.
[30] Alnaqbi AJ, Zeiada W, Al-khateeb GG, Hamad K, Barakat S. Creating rutting prediction models through machine learning techniques utilizing the long-term pavement performance database. Sustainability. 2023; 15(18):1-31.
[31] Hu X, Ishaq A, Khattak A, Chen F. Assessment of factors affecting pavement rutting in Pakistan using finite element method and machine learning models. Sustainability. 2024; 16(6):1-24.
[32] Li L, Huang X, Han D, Dong M, Zhu D. Investigation of rutting behavior of asphalt pavement in long and steep section of mountainous highway with overloading. Construction and Building Materials. 2015; 93:635-43.
[33] Patel A, Singh V, Shanker R. FEM based parametric analysis for investigating effect of wheel base characteristics and axle configurations on flexural stresses in rigid pavements. Materials Today: Proceedings. 2022; 65:1280-9.
[34] Akram HA, Hilal MM, Fattah MY. Numerical simulation of the effect of repeated load and waste polypropylene on the behavior of asphalt layers. In conference series: earth and environmental science 2022 (pp. 1-13). IOP Publishing.
[35] Li H, Guo R, Wang W. A multiphase hybrid-stress finite element method for macroscopic and microscopic modeling of composites: an element with multiple interfaces. Applied Mathematical Modelling. 2023; 116:147-67.
[36] Congress IR. IRC: 37: 2018-guidelines for the design of flexible pavements. IRC, New Delhi, India. 2018.
[37] Kumar A, Sinha S. Support vector machine-based prediction of unconfined compressive strength of multi-walled carbon nanotube doped soil-fly ash mixes. Multiscale and Multidisciplinary Modeling, Experiments and Design. 2024; 7(6):5365-86.
[38] Kashyap R, Chauhan VB, Kumar A, Jaiswal S. Machine learning-based stability assessment of unlined circular tunnels under surcharge loading. Asian Journal of Civil Engineering. 2024; 25(3):2553-66.
[39] Kumar A, Sinha S, Saurav S. Random forest, CART, and MLR-based predictive model for unconfined compressive strength of cement reinforced clayey soil: a comparative analysis. Asian Journal of Civil Engineering. 2024; 25(2):2307-23.
[40] Kumar A, Sinha S, Pandey D, Maurya MC, Chauhan VB. Advanced regression models for assessing the strength of multi-walled carbon nanotube-modified high-volume fly ash concrete. Asian Journal of Civil Engineering. 2024; 25(2):2247-68.
[41] Kumar A, Sinha S, Saurav S, Chauhan VB. Prediction of unconfined compressive strength of cement–fly ash stabilized soil using support vector machines. Asian Journal of Civil Engineering. 2024; 25(2):1149-61.

Mr. Amit Kumar holds a postgraduate degree in Transportation Engineering and is currently pursuing a Ph.D. at Dr. A.P.J. Abdul Kalam Technical University, Lucknow, Uttar Pradesh, India. He is presently working as an Assistant Professor in the Department of Civil Engineering at Rajkiya Engineering College, Azamgarh, India.
Email: amitkumar@gecazamgarh.ac.in

Mr. Rajesh Ranjan holds a postgraduate degree in Transportation Engineering and is currently pursuing a Ph.D. at the National Institute of Technology, Patna, Bihar, India.
Email: rajeshr.ph21.ce@nitp.ac.in

Dr. Anish Kumar holds a doctorate in Civil Engineering and has published extensively in prestigious journals such as ASCE, Springer, and Elsevier. His research interests include exploring novel sustainable building materials and applying artificial intelligence (AI) and machine learning (ML) to civil engineering problems. He is currently serving as an Assistant Professor in the Department of Civil Engineering at Rajkiya Engineering College, Azamgarh, Uttar Pradesh, India.
Email: anish@gecazamgarh.ac.in

Prof. Sanjeev Sinha holds a doctorate in Civil Engineering and has successfully supervised several master's and doctoral theses. He has authored multiple high-impact journal papers and is currently serving as a Professor in the Department of Civil Engineering at the National Institute of Technology, Patna, Bihar, India.
Email: sanjeev@nitp.ac.in

Appendix I

S. No.	Abbreviation	Description
1	AI	Artificial Intelligence
2	ANN	Artificial Neural Networks
3	CBR	California Bearing Ratio
4	CNN	Convolutional Neural Network
5	E	Elastic Modulus
6	FEA	Finite Element Analysis
7	FEM	Finite Element Model
8	GBDT	Gradient Boosting Decision Tree
9	GPR	Gaussian Process Regression
10	GSB	Granular Sub Base
11	HMA	Hot Mix Asphalt
12	KS	Kolmogorov-Smirnov
13	LGBM	Light Gradient Boosting Machine

14	LTPP	Long Term Pavement Performance
15	MAE	Mean Absolute Error
16	ML	Machine Learning
17	MORTH	Ministry of Road Transport and highways
18	MSE	Mean Squared Error
19	MEPDG	Mechanistic-Empirical Pavement Design Guide
20	MSLE	Mean Squared Logarithmic Error
21	RBF	Radial Basis Function
22	RMSE	Root Mean Squared Error
23	RMSLE	Root Mean Squared Logarithmic Error
24	RNN	Recurrent Neural Networks
25	SVM	Support Vector Machine
26	WBM	Water Bound Macadam
27	WMM	Wet Mix Macadam